Advances in Materials Research, *Vol. 10, No. 2 (2021) 77-98*
DOI: https://doi.org/10.12989/amr.2021.10.2.077

Analysis and sizing of RC beams reinforced by external bonding of imperfect functionally graded plate

Benferhat Rabia [1,2], Tahar Hassaine Daouadji*[1,2] and Rabahi Abderezak [1,2]

[1] *Laboratory of Geomatics and sustainable development, University of Tiaret, Algeria*
[2] *Department of Civil Engineering, Ibn Khaldoun University of Tiaret, Algeria*

(*Received March 26, 2020, Revised September 23, 2020, Accepted January 27, 2021*)

Abstract. An analytical method based on the compatibility of deformations and equilibrium of forces is investigated to predict the reinforcement plate area in concrete beams strengthened with Functionally Graded (FG) plates bonded to the tension face of the beams. The models are given for beams having rectangular and T-cross-sections. The effect of porosity that can happen inside FGM materials during their manufacture is also shown. New rules of the mixture that take into account different distribution rates of porosity in FG plates have been developed in this study. A parametric study is conducted to investigate the effect of several parameters such as the ultimate moment, plate stiffness, the distribution rate of the porosity, and compressive strength of the concrete. The results obtained show a significant gain in the reinforcement plate area of the RC beam strengthened with an FG plate relative to another reinforced with FRP plate, which makes it possible to reduce the interfacial stresses and prevents detachment of the reinforcing plate.

Keywords: RC beam; reinforcement; FGM plate; porosity

1. Introduction

Since their first use, reinforcement techniques of RC structures using composite materials have demonstrated excellent performance and have proved to be much more effective, reliable, and competitive compared to traditional reinforcement methods. The introduction in the civil engineering field of these fiber-reinforced polymers (FRP) composite materials has many functional advantages such as the lightness of the fabric, easy implementation, and freedom of shape. Although the bonding of external plates to the existing surface of reinforced concrete structures has been widely accepted as an effective technique for leveling the structure, there are few independent design guidelines and corresponding regulations.

The prediction of the flexural strength of RC beams is still a big challenge in the structural engineering domain, and specifically when FRP materials are utilized as flexural strengthening. There is not still a consensus on the evaluation of the bending strength contribution of the reinforcement FRP plate to the total bending strength. This is mainly due to the complexity of the bending phenomenon (Daouadji 2017).

According to Ashour (2002), the ultimate flexural strength of beams externally strengthened by

*Corresponding author, Professor, E-mail: daouadjitahar@gmail.com

http://www.techno-press.org/?journal=amr&subpage=5 ISSN: 2234-0912 (Print), 2234-179X (Online)

the FRP plate can be obtained as the sum of the contribution of the different components: concrete, longitudinal steel, and FRP external reinforcement. However, the interaction between all aforementioned components is not clear enough. The presence of the FRP could influence the effective stress in the internal steel reinforcement due to possible changes in the strut orientation or additional cracking that may change the relative contribution of each individual contribution to the resulting flexural strength. Guo *et al*. (2020) proposed a new improved prediction model and this model is compared by gathering results from nine RC beams strengthened with FRP grids from other literature studies. The results of this analytical model have a poor fit with the test results, especially in the situation of debonding damage. Sharaky *et al*. (2018) suggested a new technique, mechanical interlocking with shear connectors to improve the behavior in front of the failure caused by concrete cover separation or splitting. The NSM FRP strengthened RC beams showed an increment in their steel reinforcement yielding load, ranging from 30% to 60% with a marginal confinement effect. Oller *et al*. (2019) presented an experimental program of T-beams externally strengthened in shear by CFRP sheets in a discontinuous or continuous U-shaped configuration with different ratios of CFRP. The FRP sheets are not effective if they are not anchored, since a premature debonding takes place. The existence of anchorages at the end of the FRP sheets delays or avoids debonding, showing a better performance. The model proposed by Rao and Injaganeri (2011) to predict the ultimate shear strength is simple and predicts the shear strength of RC beams with a fair degree of accuracy on the deep, short and normal beams for a wide range of values of the influencing parameters. Fareed (2014) used externally bonded FRP wraps instead of strips to strengthen RC beams in flexure with and without end anchorages. It was found that the RC beams wrapped with CFRP at the bottom and extended at sides provided with and without ends anchorages, improved the structural performance of the beams in terms of stiffness, load-carrying capacity, and ductility. Al Amery and Al-Mahaidi (2006) investigated the combined shear-flexural strengthening of RC beams. It was found that a significant improvement in the beam strength up to 95% is gained due to the use of CFRP strips to anchor the CFRP sheets. It was found that the dominant mode of failure observed in the beams with strips was a ductile flexural failure with excessive yielding of internal steel prior to the rupture of CFRP sheets and crushing of the concrete. Gao *et al*. (2016) developed a new strengthening technique for strengthening RC beams with pre-tensioned CFRP laminates. It was shown that the use of pre-tensioning significantly increases the working strain of laminates assured the efficient use of material strength of CFRP laminates. The existence of a concrete pre-compressive zone delayed the crack onset and decreased crack width. Murthy *et al*. (2018) predicted the flexural behavior of reinforced concrete (RC) beams strengthened with a precast strip of ultra-high-performance fiber-reinforced concrete (UHPFRC). Ameur *et al*. (2009) shown that the level and concentration of interfacial stresses are considerably influenced by the thickness of the FRP plate. The interfacial stresses decrease as the thickness of the FRP plate decreases. Therefore, the reduction of interface stresses reduces the risk of the reinforcement plate detachment. Daouadji *et al*. (2016b) analyzed the problem of interfacial stresses in steel beams strengthened with a fiber-reinforced polymer plate using linear elastic theory. The analysis is based on the deformation compatibility approach where both the shear and normal stresses are assumed to be invariant across the adhesive layer thickness. Rabahi *et al*. (2016) proposed a simplified analytical and numerical approach to predict the interfacial stress of simply supported reinforced-concrete beams reinforced with pre-stressed carbon-fiber-reinforced polymer composite plate. Kim *et al*. (2017) investigated the effect of the CFRP (Carbon Fiber Reinforced Polymer) strengthening to the normal concrete beams. The strengthening of the beams was applied with the variation of the width and spacing of the strengthening CFPR wrapping.

Ashour (2006) gives the reports of test results of 12 concrete beams reinforced with glass fiber-reinforced polymer (GFRP) bars subjected to a four-point loading system. All test specimens had no transverse shear nor compression reinforcement and were classified into two groups according to the concrete compressive strength.

The Functionally Graded Materials (FGM) made of a mixture of metal and ceramic attract a lot of attention in the last years of their high strengths and stiffness combined with low density compared to bulk materials which allow a reduction of weight in the finished part and that justifies the need to use them for the rehabilitation of civil engineering works. However, in FGM fabrication, microvoids or porosities can occur within the materials during the process of sintering. This is because of the large difference in solidification temperatures between material constituents (Rabia *et al*. 2020a, b, Zhu *et al*. 2001, Abderezak *et al*. 2018, Belkacem *et al*. 2018, Rabia *et al*. 2019, Daouadji *et al*. 2016a, Abdelhak *et al*. 2016, Abdedezak *et al*. 2018b, Benhenni *et al*. 2019, Adim *et al*. 2016b, Hadji *et al*. 2015, Daouadji 2013, Adim and Daouadji 2016, Adim *et al*. 2016a, Abderezak *et al*. 2020, Tlidji *et al*. 2021, Bensattalah *et al*. 2018 and Abderezak *et al*. 2019). Wattanasakulpong (Wattanasakulpong *et al*. 2012 and Wattanasakulpong and Ungbhakornb 2014) also gave the discussion on porosities happening inside FGM samples fabricated by a multi-step sequential infiltration technique (Benferhat *et al*. 2016b, Benhenni *et al*. 2018, Adim *et al*. 2016c, Tayeb and Daouadji 2020, Aicha *et al*. 2020, Tahar *et al*. 2020, Hamrat *et al*. 2020, Bensattalah *et al*. 2020, Chergui *et al*. 2019, Chaded *et al*. 2018, Hadj *et al*. 2019, Daouadji *et al*. 2008, Benferhat *et al*. 2016a, Rabahi *et al*. 2016). Therefore, it is important to take into account the porosity effect and its distribution rate in the study of the concrete beam strengthened with an FG plate.

The current work presents an analytical method to predict the reinforcement plate area of concrete beam reinforced with external bonding of Functionally Graded (FG) plates. The method is based on the same principles as those adopted in the regulations concerning the flexural strength of conventional RC beams but extended here to take into account the FGM reinforcement plate. It is well known that the effect of porosity on the dimensioning of the reinforcing plate taken into account in this study is neglected in the previous works. The latter is taken into account by the use of a new modified rule of the mixture which takes into account the variation of the distribution rate of porosity.

2. Compatibility conditions

Consider a rectangular reinforced concrete section of width b and height h, reinforced:

- By longitudinal traction of steels of section A_s and height "d" to the tensest face.
- By longitudinal compression of steels of section A'_s and height "d" to the most compressed faces.
- By an FGM band of section A_{FGM} and height "d_{FGM}" to the tensest face.

The reinforcing plate is considered in FGM consisting of a mixture of metal and ceramic, wherein the composition varies from the top to the bottom surface. The upper and lower surface material is ceramic and metal, respectively.

The material properties of the reinforcement FG plates are assumed to vary continuously through the thickness of the plate. In this investigation, the imperfect plate is assumed to have porosities spreading within the thickness due to defects during production. Consider an imperfect FGM with a porosity volume fraction, α ($\alpha < 1$), distributed evenly among the metal and ceramic,

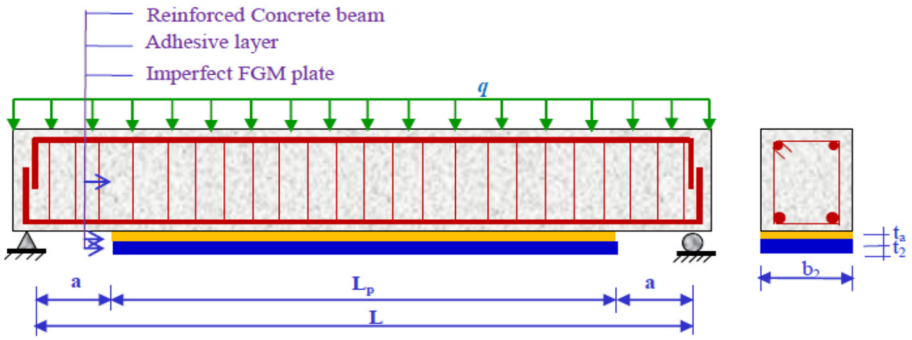

Fig. 1 Simply supported RC beam strengthened with bonded FG plate

the modified rule of mixture proposed by Wattanasakulpong and Ungbhakornb (2014) is used as

$$E(z) = E_c\left(V_C - \frac{\alpha}{2}\right) + E_m\left(V_m - \frac{\alpha}{2}\right) \tag{1}$$

Now, the total volume fraction of the metal and ceramic is: $V_m + V_c = 1$, and the power law of volume fraction of the ceramic is described as

$$V_C = \left(\frac{z_p}{h_p} + \frac{\alpha}{2}\right)^k \tag{2}$$

Hence, the Young modulus of the imperfect FGM plate can be written as an Eq. (3a). Wattanasakulpong and Ungbhakornb (2014) considered that the pores are distributed in an identical way in ceramic and metal (50%-50%). For a non-identical distribution of porosity, the new rules of mixture become like the Eqs. (3b), (3c), (3d) et (3e) (Table1).

Table 1 Summary table which groups the different distribution of porosity in the FGM (Ceramic / Metal)

Type	Porosity distribution rate		Young modulus	
	Ceramic	Metal		
Type-I	50%	50%	$E(z) = (E_c - E_m)\left(\frac{z_p}{h_p} + \frac{1}{2}\right)^k + E_m - (E_c + E_m)\frac{\alpha}{2}$	(3a)
			Wattanasakulpong *et al*. (2014)	
Type-II	60%	40%	$E(z) = (E_c - E_m)\left(\frac{z_p}{h_p} + \frac{1}{2}\right)^k + E_m - (3E_c + 2E_m)\frac{\alpha}{5}$	(3b)
Type-III	40%	60%	$E(z) = (E_c - E_m)(\frac{z_p}{h_p} + \frac{1}{2})^k + E_m - (2E_c + 3E_m)\frac{\alpha}{5}$	(3c)
Type-IV	75%	25%	$E(z) = (E_c - E_m)\left(\frac{z_p}{h_p} + \frac{1}{2}\right)^k + E_m - (3E_c + E_m)\frac{\alpha}{4}$	(3d)
Type-V	25%	75%	$E(z) = (E_c - E_m)\left(\frac{z_p}{h_p} + \frac{1}{2}\right)^k + E_m - (E_c + 3E_m)\frac{\alpha}{4}$	(3e)

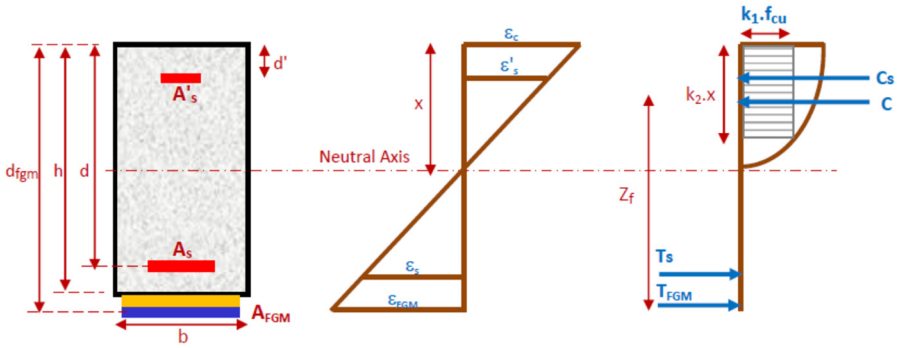

Fig. 2 Rectangular section of a reinforced concrete beam reinforced by composites: geometry, deformations distribution diagram, stresses and forces

E_c and E_m are the Young moduli of the ceramic and metal. h_p is the thickness of the reinforcement plate. k is the power-law index that takes values greater than or equal to zero. The FGM plate is a fully ceramic plate when k is set to zero and completely metallic for a large value of k.

2.1 Rectangular beam

Based on Navier Bernoulli's hypothesis, straight sections, which are planes before deformation remain plane after deformation, hence the deformation diagram is represented by a line and the deformation of fiber is proportional to its distance from the neutral axis represented by x. Let us consider the similar triangles in the deformation diagram (Fig. 2).

$$\varepsilon_S = \frac{d - x}{x}\varepsilon_C \tag{4a}$$

$$\varepsilon_S^{'} = \frac{x - d'}{x}\varepsilon_C \tag{4b}$$

$$\varepsilon_{FGM} = \frac{d_{FGM} - x}{x}\varepsilon_C \tag{4c}$$

With: ε_s : deformation of tensioned steel
ε_s' : deformation of compressed steel
ε_c : deformation of concrete
ε_{FGM} : deformation of FGM plates

$$\phi = \frac{x}{d_{FGM}} \tag{4d}$$

φ is a parameter characteristic of the state of deformation of the section.

Equilibrium conditions

The parabolic distribution of the stresses in the concrete (Fig. 1), is replaced by equivalence to

a rectangular distribution, defined by the parameters k_1 and k_2

Concrete compression force:

$$c = k_1.k_2.f_{CU}.b.x \tag{5}$$

Compression force of steel:

$$c_S = A_S'.\sigma_S' \tag{6}$$

Tensile forces of steel:

$$T_S = A_S.\sigma_S' \tag{7}$$

Tensile forces of FGM plates:

$$T_{FRP} = A_{FGM}.\sigma_{FGM} \tag{8}$$

With:

$$\sigma_{FGM} = E_{FGM}.\varepsilon_{FGM} \tag{9}$$

The equilibrium of forces

$$c + c_S = T_S + T_{FGM} \Rightarrow k_1.k_2.f_{CU}.b.x + A_S'.\sigma_S' = A_S.\sigma_S + A_{FGM}.\sigma_{FGM} \tag{10}$$

The equilibrium of moments

The bending moment *Mu* is given as

$$M_U = k_1.k_2.f_{CU}.b.x.z_{FGM} + A_S'.\sigma_S'(d_{FGM} - d') - A_S.\sigma_S(d_{FGM} - d) \tag{11}$$

$$M_U = A_{FGM}.\sigma_{FGM}.z_{FGM} + A_S'.\sigma_S'(0.5.k_2.x - d') + A_S.\sigma_S(z_{FGM} - d'') \tag{12}$$

The z_{FGM} lever is equal to

$$z_{FGM} = d_{FGM} - 0.5k_2.x = d_{FGM}(1 - 0.5.k_2.\phi) \tag{13}$$

With

$$x = \phi.d_{FGM} \tag{14}$$

From the above expression (10)

$$M_U = k_1.k_2.f_{CU}.b.x.z_F + A_S'.\sigma_S'(d_F - d') - A_S.\sigma_S(d_F - d) \tag{15}$$

Or

$$\frac{M_U + A_S\sigma_S(d_{FGM} - d) - A_S'\sigma_S'(d_{FGM} - d')}{b.d^2{}_{FGM}.k_1.f_{CU}} = k_2\phi(1 - 0.5k_2\phi) \tag{16}$$

This quantity is called the reduced moment

$$\mu = \frac{M_U + A_S\sigma_S(d_{FGM} - d) - A_S{'}\sigma_S{'}(d_{FGM} - d')}{b.d_{FGM}^2.k_1.f_{CU}} = k_2\phi(1 - 0.5k_2\phi) \tag{17}$$

Is also expressed by a second-degree equation in α which once resolved gives us

$$\mu = k_2\phi - 0.5{k_2}^2\phi^2 \Rightarrow 0.5\phi{k_2}^2 - k_2\phi + \mu = 0 \tag{18}$$

$$\phi = \frac{k_2 - \sqrt{{k_2}^2 - 2{k_2}^2\mu}}{{k_2}^2} \tag{19}$$

Where

$$\beta = 1 - 0.5k_2\phi \tag{20}$$

From the equilibrium of the moment, the reinforcement plate area is obtained as

$$A_{FGM} = \frac{M_U - A_S\sigma_S(z_{FGM} - d'') - A_S{'}\sigma_S{'}(0.5k_2x - d')}{\sigma_{FGM}.z_{FGM}} \tag{21}$$

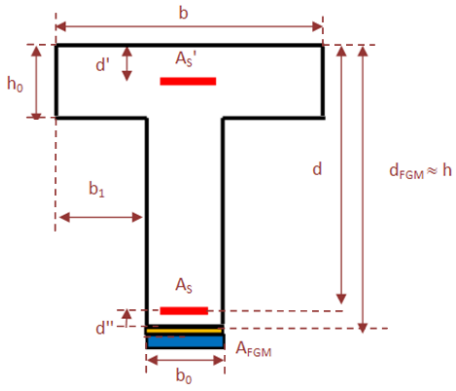

Fig. 3 Geometry of T-beam reinforced by FGM plate

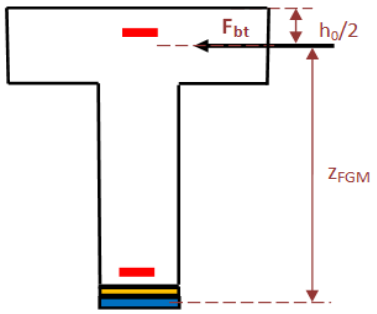

Fig. 4 Analysis of a RC T-beam reinforced with FGM plate

With

$$\sigma_{FGM} = E_{FGM}.\varepsilon_{FGM} \tag{22}$$

2.2 T- Beam

For the dimensioning of the reinforcement plate area of the T-beam, the following steps will be adopted

$$\left.\begin{array}{l} N_{bc} = K_1 f_{bc} b h_0 \\ N_S = A_S \sigma_S \\ z_{FGM} = h - \dfrac{h_0}{2} \end{array}\right\} \longrightarrow M_t = K_1 f_{bc} b h_0 \left(h - \frac{h_0}{2}\right) - A_S \sigma_S (h - d) \tag{23}$$

1st case: If $Mu \leq Mt$: The web is not fully compressed. The dimensioning will be identical to a rectangular beam ($b \times h$).

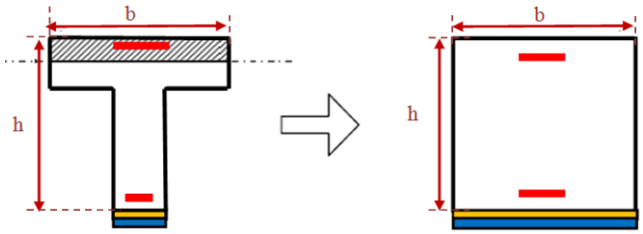

2nd case: If $Mu \geq Mt$: The web is fully compressed. The dimensioning of the composite will be by decomposing the T-section as follows

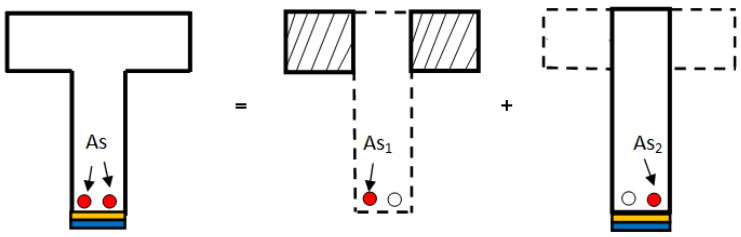

The moment balanced by the overflows

$$M_d = 2\left[\frac{b - b_0}{2}\right] h_0 k_1 f_{CU} \left(d - \frac{h_0}{2}\right) \tag{24}$$

$$M_d = (b - b_0) h_0 k_1 f_{CU} \left(d - \frac{h_0}{2}\right) \tag{25}$$

$$As_1 = \frac{M_d}{\sigma_S \left(d - \frac{h_0}{2}\right)} \tag{26}$$

The moment balanced by section b0xh
The residual moment will be

$$M_R = M_u - M_d \tag{27}$$

$$A_{S2} = A_S - A_{S1} \tag{28}$$

The expression of the reduced moment will be

$$\mu = \frac{M_R - A_S^{'}\sigma_S^{'}\left(d_{FGM} - d^{'}\right) + A_{S2}\sigma_S(d_{FGM} - d)}{b_0.d_{FGM}^2.k_1.f_{CU}} \tag{29}$$

μ: also expressed by a second-degree equation in η which once solved gives us

$$\eta = \frac{k_2 - \sqrt{k_2^2 - 2k_2^2.\mu}}{k_2^2} \tag{30}$$

with

$$\beta = 1 - 0.5k_2.\eta \tag{31}$$

FGM is equal to

$$z_{FGM} = d_{FGM}.\beta \tag{32}$$

The position of the neutral axis is defined by

$$x = \eta.d_{FGM} \tag{33}$$

Finally, the reinforcement plate area will be

$$A_{FGM} = \frac{M_R - A_{S2}\sigma_S\left(z_{FRP} - d^{''}\right) - A_S^{'}\sigma_S^{'}\left(0.5k_2.x - d^{'}\right)}{\sigma_{FGM}.z_{FGM}} \tag{34}$$

3. Results and discussions

In this section, the numerical and graphical results are presented to predict the reinforcement plate area required of a concrete beam reinforced by external bonding of the FGM plates and subjected to a static load on its upper face. The porosity effect as well as its distribution rate between the particles of the FG plate is also discussed. The properties of the materials used in this analysis (Table 2) are drawn from previous studies in the literature (Pradhan and Chakraverty 2015, Benferhat *et al*. 2016c, Tahar *et al*. 2019, Zenkour and Radwan 2018, Thai and Choi 2013 and Rabia *et al*. 2018).

Table 2 Mechanical properties of the materials used

Materials	Al_2O_3	ZrO_2	Ti-6Al-4V	Al
E (MPa)	380000	151000	105700	70000

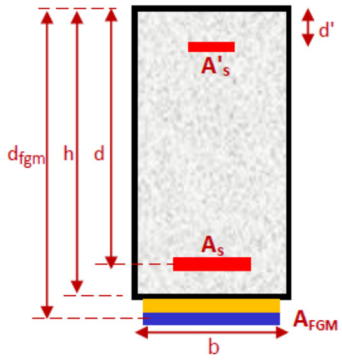

$d_{FGM} \approx h = 455$ mm | $\sigma s = 456$ N/mm^2

$k_1 = 0.67$ | $d' = 55$ mm

$E_S = 20.10^4$ N/mm^2 | $\varepsilon_{bc} = 0.0035$

$d = 400$ mm | $k_2 = 0.9$

$As = 1473$ mm^2 | $b = 205$ mm

$f_{cu} = 30$ MPa | $d'' = 55$ mm

$As' = 265.33$ mm^2

Fig. 5 Geometry of a rectangular RC beam reinforced by external bonding of the FGM plate

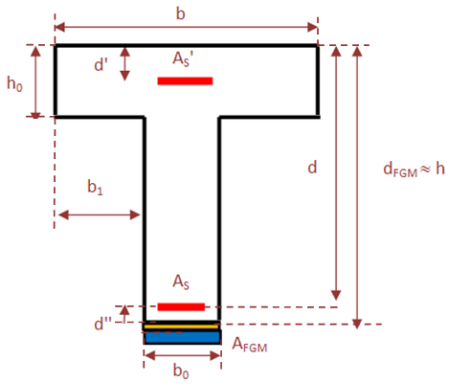

$M_u = 21117$ kN.m | $\sigma s = 400$ N/mm^2

$d_{FGM} \approx h = 1200$ mm | $d' = 100$ mm

$k_1 = 0.85$ | $\varepsilon_{bc} = 0.003$

$E_S = 20.10^3$ N/mm^2 | $k_2 = 0.85$

$d = 400$ mm | $b = 3500$ mm

$As = 44800$ mm^2 | $d'' = 100$ mm

$f_{cu} = 30$ MPa | $As' = 4800$ mm^2

$b_0 = 1200$ mm

Fig. 6 Geometry of a RC T-beam reinforced by external bonding of the FGM plates

The Poisson's ratio is taken equal to 0.3 of both alumina and aluminum. The mechanical properties of the FGM plate change through the thickness of the plate according to the power law. The geometric characteristics of the beam studied are shown in Fig. 3.

Tables 3 and 4 presents a comparison of the results of the reinforcement plate area (A_{FGM}) of a reinforced concrete beam and T-beam reinforced by external bonding of the FRP plates with another reinforced with FGM plates. The rectangular beam is reinforced on its lower part. The gradient index of the reinforcing plate in FGM is taken equal (k = 5 and 10). From these results, it can be seen that the RC beam reinforced with an FGM plate needs a smaller plate area than a beam reinforced with an FRP plate to resume the same ultimate moment applied, which makes it possible to reduce the interfacial stresses and prevents detachment of the plate according to existing studies. It can also be noted that the plate area increases when the reinforcement plate becomes richer in metal.

Table 5 shows the effect of porosity on the yield strength of the FGM plate and the reinforcement plate area of an RC beam reinforced by external bonding of the porous FGM plates. The volume fraction of porosity is considered equal to 0%, 10%, and 20%. The power-law index is taken equal (k = 2, 5, 10, and 20). Various combinations of the FGM reinforcing plate are considered to be Al/Al_2O_3, Al/ZrO_2, and Ti-6Al-4V/Al_2O_3. From this table, it can be concluded that the reinforcement plate area (A_{FGM}) increases when the reinforcement plate contains pores.

Table 3 Comparison study of the reinforcement plate area of RC beam strengthened by external bonding of FRP and FGM plates

Method	RC beam strengthened by	The reinforcement plate area of RC beam A_{FGM} (mm^2)			
Ashour (2002)	CFRP	567.837	1090.234	1834.50	2908.251
Present	CFRP	567.27	1089.87	1833,48	2907.79
	FGM, $k = 5$	263.654	506.211	851.31	1350.34
	FGM, $k = 10$	298.850	573.785	964.95	1530.599

Table 4 Comparison study of the reinforcement plate area of RC T-beam strengthened by external bonding of FRP and FGM plates

Method	RC beam strengthened by	The reinforcement plate area of RC T-beam A_{FGM} (mm^2)
Picard *et al*. 1995	CFRP	15750
Rasheed and Pervaiz 2003	CFRP	15932
Present	CFRP	15455,74
	FGM, $k = 5$	2904.35
	FGM, $k = 10$	4258.66

Table 5 Effect of the porosity on the sizing of RC beam strengthened by porous FGM plate

Reinforcing FGM plate	Porosity	$k = 2$		$k = 5$		$k = 10$		$k = 20$	
		σ_{fgm}	A_{fgm}	σ_{fgm}	A_{fgm}	σ_{fgm}	A_{fgm}	σ_{fgm}	A_{fgm}
Al/Al_2O_3	$a = 0$	561.30	459.92	303.25	851.309	267.53	964.951	266.38	969.120
	$a = 0.1$	475.68	542.71	217.62	1186.25	181.91	1419.138	180.75	1428.174
	$a = 0.2$	390.06	661.84	132.00	1955.71	96.288	2681.082	95.137	2713.516
Al/ZrO_2	$a = 0$	343.44	751.68	276.01	935.303	266.68	968.030	266.38	969.123
	$a = 0.1$	301.39	856.55	233.96	1103.404	224.63	1149.241	224.33	1150.782
	$a = 0.2$	259.34	995.44	191.91	1345.172	182.58	1413.922	182.28	1416.254
Ti-6Al-4V/Al_2O_3	$a = 0$	663.19	389.26	434.85	593.66	403.25	640.180	402.24	641.803
	$a = 0.1$	570.78	452.29	342.44	753.873	310.84	830.513	309.82	833.243
	$a = 0.2$	478.36	539.66	250.02	1032.52	218.42	1181.90	217.41	1187.4

can also be seen that the reinforcement plate area becomes larger when the reinforcement plate is Al/ZrO_2.

The effect of the geometry ratio h/b on the yield strength of the FGM plate and on the reinforcement plate area of an RC beam reinforced by external bonding of the porous FGM plates is shown in Table 6. The geometry ratio is equal (h/b = 1, 1.5 and 2). From these results, it can be seen that the square-shaped RC beam requires greater reinforcement relative to a rectangular section. It should be noted that the value of the yield strength of the FGM plate becomes lower when the reinforcement plate is porous.

Table 6 Effect of the geometry ratio h/b on the yield strength of the FGM plate and on the reinforcement plate area of an RC beam reinforced by external bonding of the porous FGM plates, $k = 5$

Reinforcing FGM plate	Porosity	$h/b = 1$		$h/b = 1.5$		$h/b = 2$	
		σ_{fgm}	A_{fgm}	σ_{fgm}	A_{fgm}	σ_{fgm}	A_{fgm}
Al/Al_2O_3	$a = 0$	1231.43	114.78	2171.53	67.60	3118.52	91.017
	$a = 0.1$	883.74	159.94	1558.40	94.20	2237.99	126.83
	$a = 0.2$	536.04	263.68	945.26	155.30	1357.47	209.09
Al/ZrO_2	$a = 0$	1120.85	126.10	1976.53	74.27	2838.46	99.99
	$a = 0.1$	950.09	148.77	1675.41	87.62	2406.03	117.96
	$a = 0.2$	779.33	181.36	1374.29	106.82	1973.59	143.82
$Ti\text{-}6Al\text{-}4V/Al_2O_3$	$a = 0$	1765.88	80.04	3113.99	47.14	4471.95	63.47
	$a = 0.1$	1390.59	101.64	2452.20	59.86	3521.58	80.59
	$a = 0.2$	1015.31	139.21	1790.42	81.98	2571.20	110.39

The effect of the compressive strength f_{cu} of the concrete on the reinforcement section of a reinforced concrete beam reinforced by external bonding of the porous FGM plates is presented in Table 7. Different values of the compressive strength of the concrete are taken into account, namely (f_{cu} = 35, 40, and 45 MPa). From the results of this table, it can be seen that the reinforcement section (A_{FGM}) becomes weaker as the compressive strength of the concrete increases. The value of the yield strength of the FGM plate is greater when the reinforcing FGM plate is $Ti\text{-}6Al\text{-}4V/Al_2O_3$. Table 8 shows the effect of the yield strength of the steel σ_e on the reinforcement section of a reinforced concrete beam reinforced by external bonding of the porous FGM plates. The yield strength of the steel is considered equal (σ_e = 300, 456, and 500 MPa). It should be noted that the section of the reinforcement decreases when the yield strength of the steel increases. The RC beam reinforced with an FGM plate needs a smaller reinforcement section when the reinforcing plate is $Ti\text{-}6Al\text{-}4V / Al_2O_3$ and larger when the reinforcement plate is Al/ZrO_2.

Table 7 Effect of the compressive strength f_{cu} of the concrete on the reinforcement section of a RC beam reinforced by external bonding of the porous FGM plates, $k = 5$

Reinforcing FGM plate	Porosity	f_{cu} = 35 MPa		f_{cu} = 40 MPa		f_{cu} = 45 MPa	
		σ_{fgm}	A_{fgm}	σ_{fgm}	A_{fgm}	σ_{fgm}	A_{fgm}
Al/Al_2O_3	$a = 0$	434.65	504.34	563.14	346.17	690.15	258.23
	$a = 0.1$	311.92	702.78	404.14	482.36	495.28	359.83
	$a = 0.2$	189.20	1158.70	245.13	795.25	300.42	593.24
Al/ZrO_2	$a = 0$	395.61	554.11	512.57	380.32	628.17	283.71
	$a = 0.1$	335.34	653.70	434.48	448.68	532.47	334.70
	$a = 0.2$	275.07	796.93	356.39	546.98	436.77	408.04
$Ti\text{-}6Al\text{-}4V/Al_2O_3$	$a = 0$	623.28	351.700	807.55	241.40	989.67	180.08
	$a = 0.1$	490.82	446.620	635.93	306.55	779.35	228.68
	$a = 0.2$	358.36	611.70	464.31	419.85	569.02	313.20

Table 8 Effect of the yield strength of steel σ_e on the reinforcement section of a reinforced concrete beam reinforced by external bonding of the porous FGM plates, $k = 5$

Reinforcing FGM plate	Porosity	σ_e = 300 MPa		σ_e = 456 MPa		σ_e = 500 MPa	
		σ_{fgm}	A_{fgm}	σ_{fgm}	A_{fgm}	σ_{fgm}	A_{fgm}
Al/Al_2O_3	$a = 0$	292.45	1578.68	303.25	851.309	306.34	655.46
	$a = 0.1$	209.87	2199.80	217.62	1186.25	219.84	913.34
	$a = 0.2$	127.30	3626.71	132.00	1955.71	133.35	1505.78
Al/ZrO_2	$a = 0$	266.18	1734.44	276.01	935.303	278.83	720.13
	$a = 0.1$	225.63	2046.1	233.96	1103.404	236.35	849.56
	$a = 0.2$	185.08	2494.51	191.91	1345.172	193.87	1035.70
$Ti\text{-}6Al\text{-}4V/Al_2O_3$	$a = 0$	419.37	1100.90	434.85	593.66	439.29	457.08
	$a = 0.1$	330.24	1397.99	342.44	753.873	345.93	345.93
	$a = 0.2$	241.12	1914.73	250.02	1032.52	252.57	794.98

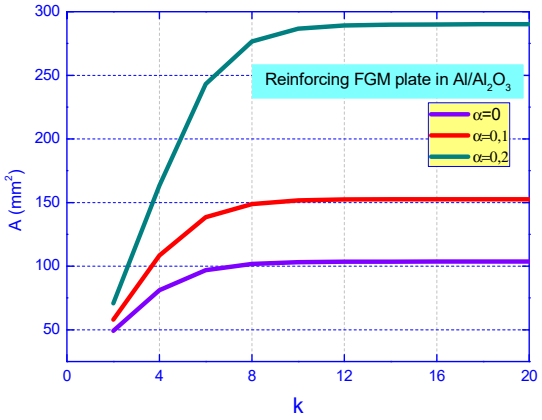

Fig. 7 Porosity effect on the sizing of a reinforced concrete beam reinforced by external bonding of a porous Al/Al_2O_3 FGM plate according to the power index

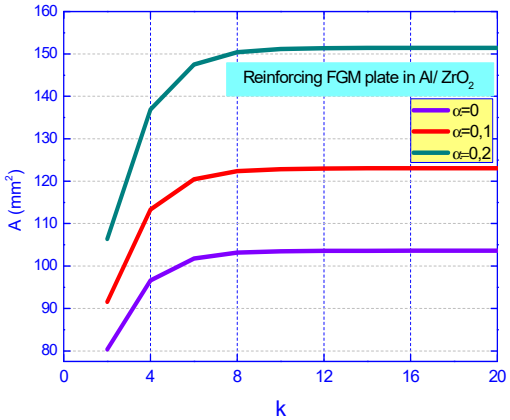

Fig. 8 Porosity effect on the sizing of a reinforced concrete beam reinforced by external bonding of a porous Al/ZrO_2 FGM plate according to the power index

Figs. 7 and 8 show the effect of porosity on the section of the reinforcement required of an RC beam reinforced by external bonding of the porous FGM plates as a function of the power-law index. The reinforcing FGM plate is considered Al/Al_2O_3, and Al/ZrO_2. The volume fraction of porosity is taken equal (α = 0, 0.1 and 0.2). From these figures, it may be noted that the section of the reinforcement becomes larger when the volume fraction of porosity and the power index increases.

The effect of the porosity distribution rate between the particles of the FGM plate on the necessary reinforcement section of a reinforced concrete beam reinforced by external bonding of the Al/Al_2O_3 and Al/ZrO_2 FGM plates as a function of the power-law index is shown in Figs. 9 and 10, respectively. The porosity rate in the FGM plate is considered equal to 20%. It can be concluded that the porosity distribution shape has a significant effect on the sizing of the reinforced concrete beam reinforced with an FGM plate. The reinforcement section becomes weaker when the porosity distribution rate is type -V.

Figs. 11 and 12 show the effect of the yield strength of the steel on the sizing of a reinforced

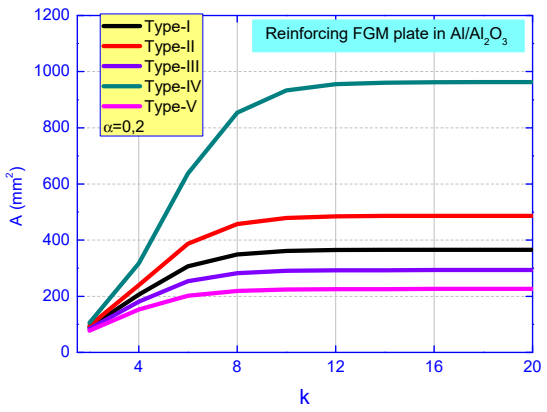

Fig. 9 Effect of the porosity distribution rate on the sizing of a reinforced concrete beam reinforced by external bonding of a porous Al/Al_2O_3 FGM plate as a function of the power index

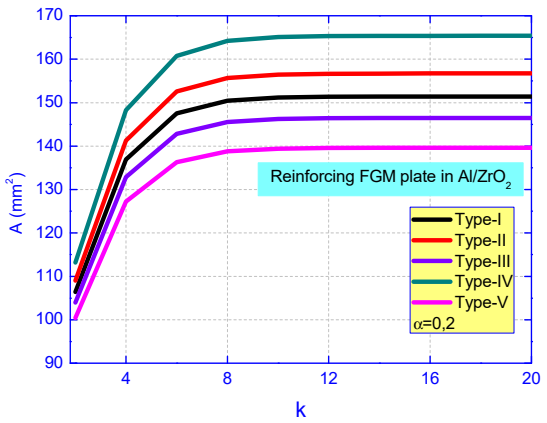

Fig. 10 Effect of the porosity distribution rate on the sizing of a reinforced concrete beam reinforced by external bonding of a porous Al/ZrO_2 FGM plate as a function of the power index

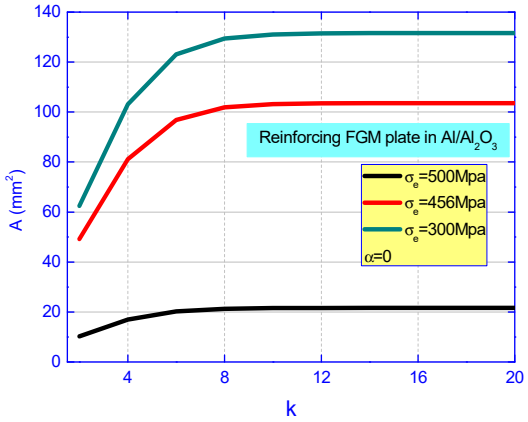

Fig. 11 Effect of the yield strength of the steel on the sizing of a reinforced concrete beam reinforced by external bonding of the FGM plates to Al / Al_2O_3 as a function of the power law index

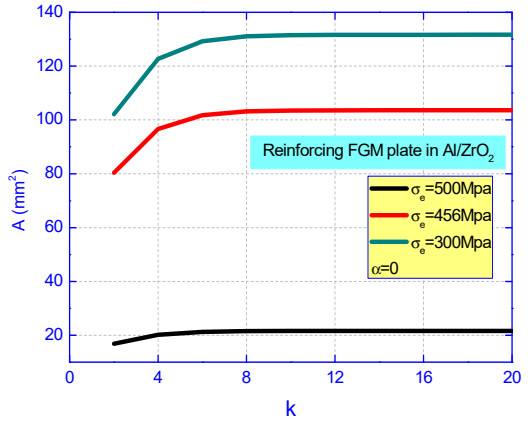

Fig. 12 Effect of the yield strength of the steel on the sizing of a reinforced concrete beam reinforced by external bonding of the FGM plates to Al/ZrO_2 as a function of the power law index

concrete beam reinforced by external bonding of the FGM plates to Al/Al_2O_3 and Al/ZrO_2 as a function of the power-law index, respectively. The FGM reinforcing plate is considered perfect (α = 0). From these figures, it can be seen that the section of the reinforcement becomes larger for the lower yield strength of the steel.

The effect of the concrete unit strain on the sizing of the reinforcement section of the RC beam reinforced by external bonding of the perfect FGM plates in Al/Al_2O_3 and Al/ZrO_2 as a function of the power-law index is shown in Figs. 13 and 14, respectively. The value of the concrete unit strain is taken equal (ε_{bc} = 3‰, 3.5‰ and 4‰). Increasing the concrete unit strain reduces the section of reinforcement required.

Figs. 15 and 16 show the influence of the compressive strength f_{cu} of the concrete on the sizing of the reinforced concrete beam reinforced by external bonding FGM plates in Al/Al_2O_3 and Al/ZrO_2, respectively. The RC beam has a rectangular shape. The compressive strength of the concrete is taken equal (f_{cu} = 30 and 40 MPa). According to these figures, it can be noted that the section of the reinforcement plate decreases with the increase in the compressive strength of the

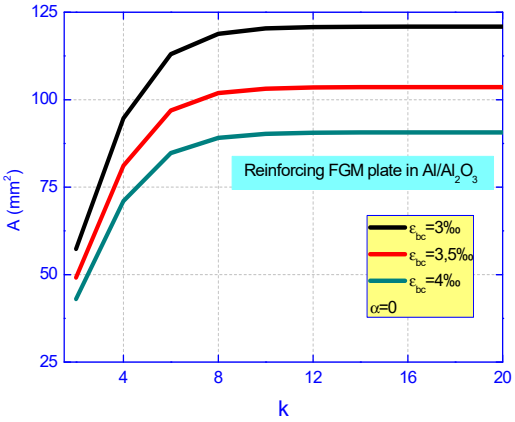

Fig. 13 Effect of the concrete unit strain on the sizing of the reinforcement section of RC beam reinforced by external bonding of the perfect FGM plates in Al/Al_2O_3 as a function of the power law index

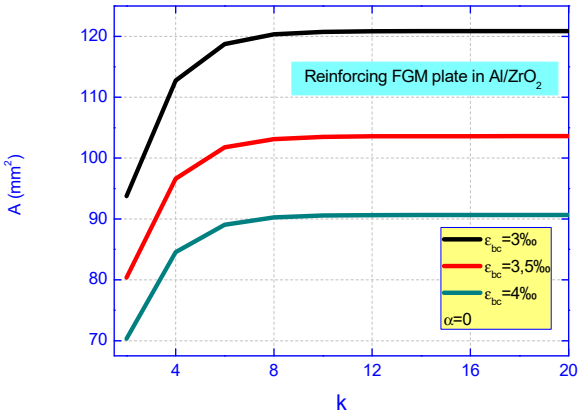

Fig. 14 Effect of the concrete unit strain on the sizing of the reinforcement section of RC beam reinforced by external bonding of the perfect FGM plates in Al/ZrO_2 as a function of the power law index

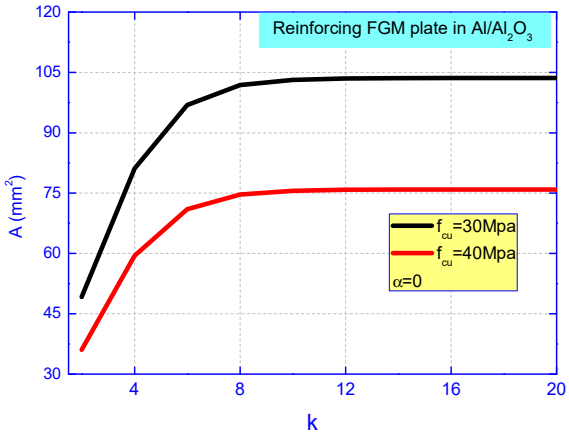

Fig. 15 Influence of the compressive strength f_{cu} of the concrete on the sizing of the reinforced concrete beam reinforced by external bonding FGM plates in Al/Al_2O_3 as a function of the power law index

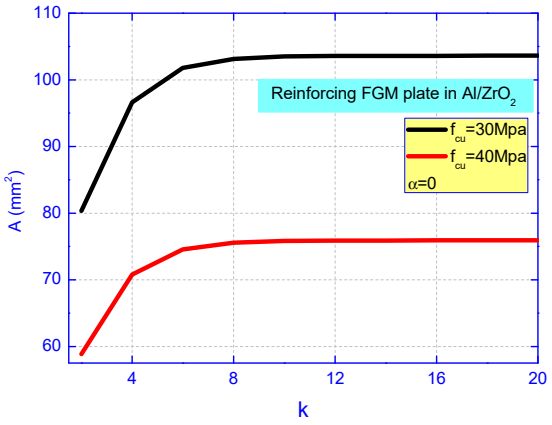

Fig. 16 Influence of the compressive strength f_{cu} of the concrete on the sizing of the reinforced concrete beam reinforced by external bonding FGM plates in Al/ZrO_2 as a function of the power law index

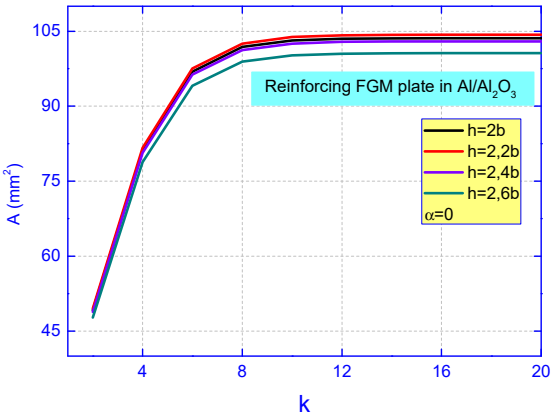

Fig. 17 Influence of the geometry ratio h/b on the reinforcement section of RC beam reinforced by external bonding of the Al/Al_2O_3 FGM plates as function of the power law index

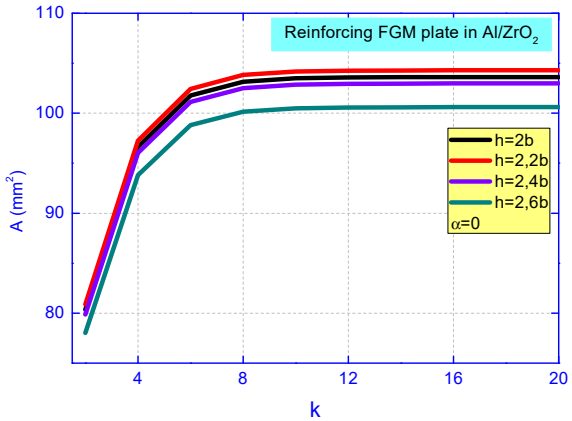

Fig. 18 Influence of the geometry ratio h/b on the reinforcement section of RC beam reinforced by external bonding of the Al/ZrO_2 FGM plates as function of the power law index

concrete.

The influence of the geometry ratio h/b on the reinforcement section of the RC beam reinforced by external bonding of the Al/Al_2O_3 and Al/ZrO_2 FGM plates as a function of the power-law index is shown in Figs. 17 and 18, respectively. These figures show that the necessary reinforcement section becomes weaker as the geometry ratio *h*/*b* increases. It can also be seen from these figures and the preceding figure that the reinforcement section increases more significantly when the power law index of the FGM plate varies from 2 to 8 and increases slightly when the latter varies from 10 at 22.

4. Conclusions

This study investigated an analytical method for predicting the reinforcement plate area of strengthening concrete beams. The reinforcement plate is considered to be made of FGM. The effect of porosity that can occur inside FGM materials during their manufacture is also shown. New rules of the mixture that take into account different distribution rates of porosity in FG plate have been developed in this work. According with numerical and graphical results, some conclusions can be drawn as follows:

- The existing porosity in the reinforcement plate increases the required plate section.
- The porosity distribution rate has a significant effect on the section of the FGM plate, it becomes smaller when the porosity distribution rate is type-V.
- The increase in the compressive strength of concrete reduces the cross-section of the plate required.
- The power-law index *k* has a significant influence on the cross-section of the reinforcing plate.
- The square-shaped RC beam requires greater reinforcement relative to a rectangular section.

Acknowledgments

This research was supported by the Algerian Ministry of Higher Education and Scientific Research (MESRS) as part of the grant for the PRFU research project n° A01L02UN140120200002 and by the University of Tiaret, in Algeria.

References

Abdelhak, Z., Hadji, L., Daouadji, T.H. and Adda Bedia, E.A. (2016), "Thermal buckling response of functionally graded sandwich plates with clamped boundary conditions", *Smart Struct. Syst.*, *Int. J.*, **18**(2), 267-291. https://doi.org/10.12989/sss.2016.18.2.267

Abderezak, R., Daouadji, T.H., Rabia, B. and Belkacem, A. (2018b), "Nonlinear analysis of damaged RC beams strengthened with glass fiber reinforced polymer plate under symmetric loads", *Earthq. Struct.*, *Int. J.*, **15**(2), 113-122. https://doi.org/10.12989/eas.2018.15.2.113

Abderezak, R., Daouadji, T.H., Abbes, B., Rabia, B., Belkacem, A. and Abbes, F. (2018b), "Elastic analysis of interfacial stress concentrations in CFRP-RC hybrid beams: Effect of creep and shrinkage", *Adv. Mater. Res.*, *Int. J.*, **6**(3), 257-278. https://doi.org/10.12989/amr.2017.6.3.257

Abderezak, R., Rabia, B., Daouadji, T.H., Abbes, B., Belkacem, A. and Abbes, F. (2019), "Elastic analysis

of interfacial stresses in prestressed PFGM-RC hybrid beams", *Adv. Mater. Res., Int. J.*, **7**(2), 83-103. https://doi.org/10.12989/amr.2018.7.2.083

Abderezak, R., Daouadji, T.H. and Rabia, B. (2020), "Analysis of interfacial stresses of the reinforced concrete foundation beams repairing with composite materials plate", *Coupl. Syst. Mech., Int. J.*, **9**(5), 473-498. http://dx.doi.org/10.12989/csm.2020.9.5.473

Adim, B. and Daouadji, T.H. (2016), "Effects of thickness stretching in FGM plates using a quasi-3D higher order shear deformation theory", *Adv. Mater. Res., Int. J.*, **5**(4), 223-244. https://doi.org/10.12989/amr.2016.5.4.223

Adim, B., Daouadji, T.H. and Abbes, B. (2016a), "Buckling analysis of anti-symmetric cross-ply laminated composite plates under different boundary conditions", *Int. Appl. Mech.*, **52**(6), 126-141. https://doi.org/10.1007/s10778-016-0787-x

Adim, B., Daouadji, T.H., Rabia, B. and Hadji, L. (2016b), "An efficient and simple higher order shear deformation theory for bending analysis of composite plates under various boundary conditions", *Earthq. Struct., Int. J.*, **11**(1), 63-82. https://doi.org/10.12989/eas.2016.11.1.063

Adim, B., Daouadji, T.H., Abbes, B. and Rabahi, A. (2016c), "Buckling and free vibration analysis of laminated composite plates using an efficient and simple higher order shear deformation theory", *Mech. Ind.*, **17**, 512. https://doi.org/10.1051/meca/2015112

Aicha, K., Rabia, B., Daouadji, T.H. and Bouzidene, A. (2020), "Effect of porosity distribution rate for bending analysis of imperfect FGM plates resting on Winkler-Pasternak foundations under various boundary conditions", *Coupl. Syst. Mech., Int. J.*, **9**(6), 575-597. http://doi.org/10.12989/csm.2020.9.6.575

Al-Amery, R. and Al-Mahaidi, R. (2006), "Coupled flexural-shear retrofitting of RC beams using CFRP straps", *Compos. Struct.*, **75**, 457-464. https://doi.org/10.1016/j.compstruct.2006.04.037

Ameur, M., Tounsi, A., Benyoucef, S., Bouiadjra, M.B. and Bedia, E.A. (2009), "Stress analysis of steel beams strengthened with a bonded hygrothermal aged composite plate", *Int. J. Mech. Mater. Des.*, **5**, 143-156. https://doi.org/10.1007/s10999-008-9090-2

Ashour, A.F. (2002), "Size of FRP laminates to strengthen reinforced concrete sections in flexure", *Struct. Build.*, **152**(3), 225-233. https://doi.org/10.1680/stbu.2002.152.3.225

Ashour, A.F. (2006), "Flexural and shear capacities of concrete beams reinforced with GFRP bars", *Constr. Build. Mater.*, **20**, 1005-1015. https://doi.org/10.1016/j.conbuildmat.2005.06.023

Benferhat, R., Daouadji, T.H., Mansour, M.S. and Hadji, L. (2016a), "Effect of porosity on the bending and free vibration response of functionally graded plates resting on Winkler-Pasternak foundations", *Earthq. Struct., Int. J.*, **10**(6), 1429-1449. https://doi.org/10.12989/eas.2016.10.6.1429

Benferhat, R., Daouadji, T.H. and Adim, B. (2016b), "A novel higher order shear deformation theory based on the neutral surface concept of FGM plate under transverse load", *Adv. Mater. Res., Int. J.*, **5**(2), 107-120. https://doi.org/10.12989/amr.2016.5.2.107

Benferhat, R., Daouadji, T.H. and Mansour, M.S. (2016c), "Free vibration analysis of FG plates resting on the elastic foundation and based on the neutral surface concept using higher order shear deformation theory", *Comptes Rendus Mecanique*, **344**(9), 631-641. https://doi.org/10.1016/j.crme.2016.03.002

Belkacem, A., Tahar, H.D., Abderrezak, R., Amine, B.M., Mohamed, Z. and Boussad, A. (2018), "Mechanical buckling analysis of hybrid laminated composite plates under different boundary conditions", *Struct. Eng. Mech., Int. J.*, **66**(6), 761-769. https://doi.org/10.12989/sem.2018.66.6.761

Benhenni, M.A., Daouadji, T.H., Abbes, B., Adim, B., Li, Y. and Abbes, F. (2018), "Dynamic analysis for anti-symmetric cross-ply and angle-ply laminates for simply supported thick hybrid rectangular plates", *Adv. Mater. Res., Int. J.*, **7**(2), 83-103. https://doi.org/10.12989/amr.2018.7.2.119

Benhenni, M.A., Daouadji, T.H., Abbes, B., Abbes, F., Li, Y. and Adim, B. (2019), "Numerical analysis for free vibration of hybrid laminated composite plates for different boundary conditions", *Struct. Eng. Mech., Int. J.*, **70**(5), 535-549. https://doi.org/10.12989/sem.2019.70.5.535

Bensattalah, T., Zidour, M. and Daouadji, T.H. (2018), "Analytical analysis for the forced vibration of CNT surrounding elastic medium including thermal effect using nonlocal Euler-Bernoulli theory", *Adv. Mater. Res., Int. J.*, **7**(3), 163-174. https://doi.org/10.12989/amr.2018.7.3.163

Bensattalah, T., Daouadji, T.H. and Zidour, M. (2020), "Influences the Shape of the Floor on the Behavior of Buildings Under Seismic Effect", *Proceedings of the 4th International Symposium on Materials and Sustainable Development*, Volume 1 - Nano Technology and Advanced Materials, pp. 26-42. https://doi.org/10.1007/978-3-030-43268-3_3

Chedad, A., Daouadji, T.H., Abderezak, R., Adim, B., Abbes, B., Rabia, B. and Abbes, F. (2018), "A high-order closed-form solution for interfacial stresses in externally sandwich FGM plated RC beams", *Adv. Mater. Res., Int. J.*, **6**(4), 317-328. https://doi.org/10.12989/amr.2017.6.4.317

Chergui, S., Daouadji, T.H., Hamrat, M., Boulekbache, B., Bougara, A., Abbes, B. and Amziane, S. (2019), "Interfacial stresses in damaged RC beams strengthened by externally bonded prestressed GFRP laminate plate: Analytical and numerical study", *Adv. Mater. Res., Int. J.*, **8**(3), 197-217. https://doi.org/10.12989/amr.2019.8.3.197

Daouadji, T.H. (2013), "Analytical analysis of the interfacial stress in damaged reinforced concrete beams strengthened by bonded composite plates", *Strength Mater.*, **45**(5), 587-597. https://doi.org/10.1007/s11223-013-9496-4

Daouadji, T.H. (2017), "Analytical and numerical modeling of interfacial stresses in beams bonded with a thin plate", *Adv. Computat. Des., Int. J.*, **2**(1), 57-69. https://doi.org/10.12989/acd.2017.2.1.057

Daouadji, H.T., Benyoucef, S., Tounsi, A., Benrahou, K.H. and Bedia, A.E. (2008), "Interfacial stress concentrations in FRP-damaged RC hybrid beams", *Compos. Interf.*, **15**(4), 425-440. https://doi.org/10.1163/156855408784514702

Daouadji, T.H., Rabahi, A., Abbes, B. and Adim, B. (2016a), "Theoretical and finite element studies of interfacial stresses in reinforced concrete beams strengthened by externally FRP laminates plate", *J. Adhes. Sci. Technol.*, **30**(12), 1253-1280. https://doi.org/10.1080/01694243.2016.1140703

Daouadji, T.H., Hadji, L., Meziane, M.A.A. and Bekki, H. (2016b), "Elastic analysis effect of adhesive layer characteristics in steel beam strengthened with a fiber-reinforced polymer plates", *Struct. Eng. Mech., Int. J.*, **59**(1), 83-100. https://doi.org/10.12989/sem.2016.59.1.083

Fareed, S. (2014), "Behaviour of reinforced concrete beams strengthened by CFRP wraps with and without end anchorages", *Procedia Eng.*, **77**, 123-130. https://doi.org/10.1016/j.proeng.2014.07.011

Gao, P., Gu, X. and Mosallam, A.S. (2016), "Flexural behavior of preloaded reinforced concrete beams strengthened by prestressed CFRP laminates", *Compos. Struct.*, **157**(1), 33-50. https://doi.org/10.1016/j.compstruct.2016.08.013

Guo, R., Hu, W., Li, M. and Wang, B. (2020), "Study on the flexural strengthening effect of RC beams reinforced by FRP grid with PCM shotcrete", *Compos. Struct.*, **239**(1), 112000. https://doi.org/10.1016/j.compstruct.2020.112000

Hadji, L., Daouadji, T.H. and Bedia, E.A. (2015), "A refined exponential shear deformation theory for free vibration of FGM beam with porosities", *Geomech. Eng., Int. J.*, **9**(3), 361-372. https://doi.org/10.12989/gae.2015.9.3.361

Hadj, B., Rabia, B. and Daouadji, T.H. (2019), "Influence of the distribution shape of porosity on the bending FGM new plate model resting on elastic foundations", *Struct. Eng. Mech., Int. J.*, **72**(1), 823-832. https://doi.org/10.12989/sem.2019.72.1.061

Hamrat, M., Bouziadi, F., Boulekbache, B., Daouadji, T.H., Chergui, S., Labed, A. and Amziane, S. (2020), "Experimental and numerical investigation on the deflection behavior of pre-cracked and repaired reinforced concrete beams with fiber-reinforced polymer", *Constr. Build. Mater.*, **249**, 118745. http://dx.doi.org/10.1016/j.conbuildmat.2020.118745

Kim, M., Pokhrel, A., Jung, D., Kim, S. and Park, C. (2017), "The Strengthening Effect of CFRP for Reinforced Concrete Beam", *Procedia Eng.*, **210**, 141-147. https://doi.org/10.1016/j.proeng.2017.11.059

Murthy, A.R., Aravindan, M. and Ganesh, P. (2018), "Prediction of flexural behaviour of RC beams strengthened with ultra high performance fiber reinforced concrete", *Struct. Eng. Mech., Int. J.*, **65**(3), 315-325. https://doi.org/10.12989/sem.2018.65.3.315

Oller, E., Pujol, M. and Mari, A. (2019), "Contribution of externally bonded FRP shear reinforcement to the

shear strength of RC beams", *Compos*. *Part B*, **164**(1), 235-248. https://doi.org/10.1016/j.compositesb.2018.11.065.

Picard, A., Massicotte, B. and Boucher, E. (1995), "Strengthening of reinforced concrete beams with composite materials: theoretical study", *Compos. Struct.*, **33**, 63-75. https://doi.org/10.1016/0263-8223(95)00106-9

Pradhan, K.K. and Chakraverty, S. (2015), "Free vibration of functionally graded thin elliptic plates with various edge support", *Struct*. *Eng*. *Mech*., *Int*. *J*., **53**(2), 337-354. https://doi.org/10.12989/sem.2015.53.2.337

Rabahi, A., Daouadji, T.H., Abbes, B. and Adim, B. (2016), "Analytical and numerical solution of the interfacial stress in reinforced-concrete beams reinforced with bonded prestressed composite plate", *J*. *Reinf*. *Plast*. *Compos*., **35**(3), 258-272. https://doi.org/10.1177/0731684415613633

Rabia, B., Abderezak, R., Daouadji, T.H., Abbes, B., Belkacem, A. and Abbes, F. (2018), "Analytical analysis of the interfacial shear stress in RC beams strengthened with prestressed exponentially-varying properties plate", *Adv*. *Mater*. *Res*., *Int*. *J*., **7**(1), 29-44. https://doi.org/10.12989/amr.2018.7.1.029

Rabia, B., Daouadji, T.H. and Abderezak, R. (2019), "Effect of distribution shape of the porosity on the interfacial stresses of the FGM beam strengthened with FRP plate", *Earthq*. *Struct*., *Int*. *J*., **16**(5), 601-609. https://doi.org/10.12989/eas.2019.16.5.601

Rabia, B., Tahar, H.D. and Abderezak, R. (2020a), "Thermo-mechanical behavior of porous FG plate resting on the Winkler-Pasternak foundation", *Coupl*. *Syst*. *Mech*., *Int*. *J*., **9**(6), 499-519. http://doi.org/10.12989/csm.2020.9.6.499

Rabia, B., Daouadji, T.H. and Abderezak, R. (2020b), "Predictions of the maximum plate end stresses of imperfect FRP strengthened RC beams: study and analysis", *Adv*. *Mater*. *Res*., *Int*. *J*., **9**(4), 265-287. http://doi.org/10.12989/amr.2020.9.4.265

Rabahi, A., Daouadji, T.H., Abbes, B. and Adim, B. (2016), "Analytical and numerical solution of the interfacial stress in reinforced-concrete beams reinforced with bonded prestressed composite plate", *J*. *Reinf*. *Plast*. *Compos*., **35**(3), 258-272. https://doi.org/10.1177/0731684415613633

Rao, G.A. and Injaganeri, S.S. (2011), "Evaluation of size dependent design shear strength of reinforced concrete beams without web reinforcement", *Ind*. *Acad*. *Sci*., **36**(3), 393-410. https://doi.org/10.1007/s12046-011-0029-1

Rasheed, H.A. and Pervaiz, S. (2003), "Closed form equations for FRP flexural strengthening design of RC beams", *Composites*: *Part B*: *Eng*., **34**, 539-550. https://doi.org/10.1016/S1359-8368(03)00047-7

Sharaky, I.A., Baena, M., Barris, C., Sallam, H.E.M. and Torres, L. (2018), "Effect of axial stiffness of NSM FRP reinforcement and concrete cover confinement on flexural behaviour of strengthened RC beams: Experimental and numerical study", *Eng*. *Struct*., **173**, 987-1001. https://doi.org/10.1016/j.engstruct.2018.07.062.

Tahar, H.D., Boussad, A., Abderezak, R., Rabia, B., Fazilay, A. and Belkacem, A. (2019), "Flexural behaviour of steel beams reinforced by carbon fibre reinforced polymer: Experimental and numerical study", *Struct*. *Eng*. *Mech*., *Int*. *J*., **72**(4), 409-419. https://doi.org/10.12989/sem.2019.72.4.409

Tahar, H.D., Abderezak, R. and Rabia, B. (2020), "Flexural performance of wooden beams strengthened by composite plate", *Struct*. *Monitor*. *Maint*., *Int*. *J*., **7**(3), 233-259. http://doi.org/10.12989/smm.2020.7.3.233

Tayeb, B. and Daouadji, T.H. (2020), "Improved analytical solution for slip and interfacial stress in composite steel-concrete beam bonded with an adhesive", *Adv*. *Mater*. *Res*., *Int*. *J*., **9**(2), 133-153. https://doi.org/10.12989/amr.2020.9.2.133

Thai, H.T. and Choi, D.H (2013), "Finite element formulation of various four unknown shear deformation theories for functionally graded plates", *Finite Elem*. *Anal*. *Des*., **75**, 50-61. https://doi.org/10.1016/j.finel.2013.07.003

Tlidji, Y., Benferhat, R. and Tahar, H.D. (2021), "Study and analysis of the free vibration for FGM microbeam containing various distribution shape of porosity", *Struct*. *Eng*. *Mech*., *Int*. *J*., **77**(2), 217-229. http://doi.org/10.12989/sem.2021.77.2.217

Tounsi, A., Daouadji, T.H. and Benyoucef, S. (2008), "Interfacial stresses in FRP-plated RC beams: Effect

of adherend shear deformations", *Int. J. Adhes. Adhes.*, **29**, 343-351. https://doi.org/10.1016/j.ijadhadh.2008.06.008

Wattanasakulponga, N. and Ungbhakornb, V. (2014), "Linear and non linear vibration analysis of elastically restrained ends FGM beams with porosities", *Aero. Sci. Technol.*, **32**(1), 111-120. https://doi.org/10.1016/j.ast.2013.12.002

Wattanasakulpong, N., Prusty, B.G., Kelly, D.W. and Hoffman, M. (2012), "Free vibration analysis of layered functionally graded beams with experimental validation", *Mater. Des.*, **36**, 182-190. https://doi.org/10.1016/j.matdes.2011.10.049

Zenkour, A.M. and Radwan, A.F. (2018), "Compressive study of functionally graded plates resting on Winkler-Pasternak foundations under various boundary conditions using hyperbolic shear deformation theory", *Arch. Civil Mech. Eng.*, **18**, 645-658. https://doi.org/10.1016/j.acme.2017.10.003

Zhu, J., Lai, Z., Yin, Z., Jeon, J. and Lee, S. (2001), "Fabrication of ZrO2-NiCr functionally graded material by powder metallurgy", *Mater. Chem. Phys.*, **68**(1-3), 130-135. https://doi.org/10.1016/S0254-0584(00)00355-2

CC